CONF-790731--1

Charged Particle Irradiations in the United States Breeder Reactor Program*

(Contribution to US/USSR Breeder Reactor Information Exchange, 1979)

A. F. Rowcliffe, E. H. Lee, P. S. Sklad

Metals and Ceramics Division
Oak Ridge National Laboratory
Oak Ridge, Tennessee 37830

1. Introduction: The Correlation of Neutron Data with Charged Particle Irradiation Damage Data

During the past 8–9 years charged particle irradiations have been widely used as a means of studying displacement damage effects in metals and alloys. In the Breeder Reactor Program, a major concern has been to correlate the results of these studies with the behavior of alloys in-reactor. As experience with these techniques accumulated it was realized that the physical environment of a material undergoing charged particle irradiation differed significantly from that experienced in neutron irradiation experiments. Some of the important differences are:

a. The proximity of surfaces. The damaged region may be <1.0 μ from a surface which acts as a point defect sink. At high temperatures this results in the formation of void free zones, and possibly a reduction in swelling rate in the peak damage region. In very soft materials loss of dislocations to the surface may inhibit swelling. In some instances, particularly in 1 MeV electron irradiations, absorption of gases prior to or during irradiation may influence results.

b. Dose rate effects. The temperature regime for swelling and solute migration are shifted upwards, not necessarily by the same amount.

*Research sponsored by the Office of Reactor Research and Technology, U.S. Department of Energy under contract W-7405-eng-26 with the Union Carbide Corporation.

Charged Particle Irradiations in the United States Breeder Reactor Program

1. Introduction: The Correlation of Neutron Data with Charged Particle Irradiation Damage Data

During the past 8–9 years charged particle irradiations have been widely used as a means of studying displacement damage effects in metals and alloys. In the Breeder Reactor Program, a major concern has been to correlate the results of these studies with the behavior of alloys in-reactor. As experience with these techniques accumulated it was realized that the physical environment of a material undergoing charged particle irradiation differed significantly from that experienced in neutron irradiation experiments. Some of the important differences are:

a. The proximity of surfaces. The damaged region may be <1.0 μ from a surface which acts as a point defect sink. At high temperatures this results in the formation of void free zones, and possibly a reduction in swelling rate in the peak damage region. In very soft materials loss of dislocations to the surface may inhibit swelling. In some instances, particularly in 1 MeV electron irradiations, absorption of gases prior to or during irradiation may influence results.

b. Dose rate effects. The temperature regime for swelling and solute migration are shifted upwards, not necessarily by the same amount.

In heavy ion irradiations, cascade dissolution phenomena strongly influence the stability of phases.

c. Stress state. The nonuniform distribution of swelling leads to a compressive and anisotropic stress state in the damaged region of the specimen, whereas the stress state is changed very little by neutron irradiation.

d. Nonuniform damage distribution in heavy ion irradiations. The damage rate varies with depth below the surface and thus the temperature shift also varies along the ion range. In addition, as swelling increases, ion range also increases, and careful sectioning techniques and range correction procedures are needed to relate swelling to displacement dose.

e. Differences in recoil spectra. In 1 MeV electron irradiations, displacement cascades are nonexistent. The effective production rate of free defects per incident particle is much higher than in neutron or heavy ion irradiations in which a high fraction of displaced atoms are instantaneously recombined and a significant proportion of vacancies collapse to form small loops.

f. The injected interstitial effect. To avoid significant changes in alloy composition during irradiation, the ion used for damage studies should be one of the major components of the alloy being studied. The injected ions form a population of extra interstitials which significantly perturb the point defect balance in the recombination-dominated swelling regime. This has the effect of reducing swelling in the peak damage region and moving the peak swelling region towards the surface.

g. Helium injection. The continuous generation of helium in-reactor controls high temperature void nucleation. Until very recently,

charged particle irradiations have been carried out with helium preinjected at room temperature. In these circumstances, complex interactions between mobile helium and precipitation do not occur.

Some of these differences, particularly those associated with displacement rate computations, damage rate gradients, stress effects, injected interstitials and recoil spectra, may be accounted for in terms of a "dose equivalence" [1]. Such an equivalence factor may be experimentally determined by comparing the number of displacements per atom (dpa) required to produce the same amount of void swelling in each environment at the peak swelling temperature. It is now realized that swelling behavior in complex alloys is controlled to a large extent by the development of precipitate phases during irradiation [2]. However, the development of precipitate phases does not necessarily follow the same temperature and dose dependency in environments with different damage rates. This being so, the use of a dose equivalence concept to relate charged particle and neutron results is only of limited value. To investigate the question of the relationship between charged particle and neutron irradiations, a comprehensive experiment was carried out utilizing a single heat (M2783) of solution annealed AISI 316 stainless steel, Table 1, which had been irradiated in EBR-II to fluences of up to $\sim 12 \times 10^{22}$ n·cm^{-2} (E > 0.1 MeV) [3]. The evolution of the void, dislocation, and precipitate components of the microstructure were determined by analytical transmission electron microscopy (TEM) for irradiation temperatures of 450 and 585°C. Nickel ion irradiations were carried out on archive specimens of the same material, preinjected with 5 appm helium at room temperature. Ni ion irradiations were then performed on specimens which had been previously irradiated in-reactor to a fluence of 8×10^{22} n·cm^{-2}. This preconditioning procedure was adopted to establish the in-reactor precipitate structure, and void and dislocation sink strengths, before commencing the charged particle irradiations. A description of this experiment and the impact of its results is the main subject of this contribution.

2. Neutron Irradiation of SA 316 Stainless Steel

Following an anneal at 1090°C, specimens were irradiated in the EBR-II X098 subassembly in the form of tubes 6.35 mm OD and 0.38 mm wall thickness. Swelling, derived from profilometry data, is plotted as a function of irradiation temperature in Fig. 1. This material exhibits a swelling peak at 585°C with a swelling rate of $2.7\%/10^{22}$ n·cm^{-2}. The data suggests that a second peak occurs at 450°C with a swelling rate of $0.9\%/10^{22}$ n·cm^{-2}. (Double peak swelling behavior in SA 316 has also been reported, for example, by Bramman et al. [4].) Typical microstructures after irradiation to 8×10^{22} n·cm^{-2} are presented in Fig. 2, and the microstructural data is shown in Table 2. At 450°C precipitation consisted of a small number density of carbide particles ∿30 nm diam of an undetermined nature, and a fairly uniform dispersion of γ′ particles ($L\ell_2$ structure). These particles were ∿10 nm diam and their number density ∿10^{15} particles cm^{-2}. Their composition was determined to be Ni_3Si by analytical TEM. At 585°C the microstructure was dominated by voids >100 nm diam associated with plate shaped precipitates of comparable dimensions. A family of smaller voids, not associated with precipitates was also present. At this temperature the γ′ phase could not be detected. The plate shaped phase was shown to have a FCC structure with a lattice parameter ∿1.1 nm, i.e., it was isostructural with $M_{23}C_6$. Energy dispersive x-ray analysis of particles extracted on carbon films showed that the composition of these particles, in wt %. was 15 Fe–32 Cr–33 Ni–14 Mo–6 Si. During thermal aging of SA316 in the range 450–900°C, the principal phase formed is an $M_{23}C_6$ with an approximate composition 18 Fe–63 Cr–14 Mo–5 Ni [5]. Other phases which occur are η, χ, and σ; γ′ does not occur during thermal aging. Thus during neutron irradiation, radiation-induced and radiation-enhanced precipitation occurs of phases which are rich in nickel and silicon. The precipitation of these phases exerts a strong influence on the temperature dependence of swelling. The formation of

γ' at ~450°C occurs as the result of the segregation of Ni and Si induced by the flow of point defects towards sinks. The mechanisms of segregation have been investigated in other experiments [6,7]. The removal of these elements from solution results in a decrease in swelling resistance and the formation of a swelling peak at ~450°C coinciding with a maximum in the rate of formation of γ'. The amount of $M_{23}C_6$ formed in reactor at 585°C is enhanced above that formed during thermal aging and this phase becomes highly enriched in nickel and silicon at the expense of chromium. This compositional modification is also the result of point defect flow-induced segregation and the nickel and silicon content of the matrix is substantially reduced. In addition, the particle-matrix interface acts as an efficient trap for helium and facilitates the nucleation of stable voids which grow rapidly in association with the particles. This precipitation phenomenon is believed to control the formation of the in-reactor swelling peak at ~585°C.

3. 4 MeV Ni Ion Irradiations of SA316

Discs, 3 mm diam, were spark cut from unirradiated tubes and the surfaces carefully prepared for charged particle irradiations. Helium was preinjected at room temperature to a level of 5 appm. Ion irradiations were carried out at a displacement rate of 4×10^{-3} dpa s^{-1} to a peak dose of 100 dpa (calculated using the EDEP-1 code and a value of 40 eV for the effective threshold energy). A single peaked swelling curve was observed with maximum swelling occurring at ~650°C, Fig. 3. The γ' and massive $M_{23}C_6$ phases which formed during reactor irradiation were not observed at any temperature in the ion irradiations, and precipitation was limited to a very small volume fraction of carbides ~20 nm diam, Fig. 4. The steady state void number densities in reactor at 450 and 585°C were ~5×10^{14} cm^{-3} and ~3×10^{13} cm^{-3}, respectively. Under ion irradiation, the void number densities were in a similar range and decreased from 9×10^{14} cm^{-3}

at 550°C to 8 × 10^{13} cm^{-3} at 700°C. Further experiments were carried out with SA316 specimens in which α-particles with continuously varying energy were introduced simultaneously with 4 MeV Ni ions to produce a uniform distribution of helium in the ion damage region. Using a rate of 0.4 appm/dpa, double peaked swelling behavior was not observed although the swelling range was extended to higher temperatures, Fig. 3. Precipitation behavior was unaffected by the simultaneous introduction of helium.

The evidence is very convincing that the temperature dependence of in-reactor swelling and the swelling rate is largely controlled by phase instability and its effects on matrix chemistry and by the interaction between helium and incoherent or partially coherent particles. In SA316, these phase changes do not occur in the high damage rate regimes of charged particle experiments, and it is concluded that this is the major factor which prevents the proper simulation of either the temperature dependence or dose dependence of in-reactor swelling.

4. 4 MeV Ni Ion Irradiations on Neutron Preconditioned Specimens

After irradiation to a fluence of ∿8 × 10^{22} $n \cdot cm^{-2}$, the evolution of the precipitate microstructure in SA316 has reached a steady state situation, and swelling proceeds at constant void number density, Table 2. Specimens in this condition were subjected to further heavy ion irradiations and swelling determined as a function of dose at several temperatures. Nickel ion irradiation swelling results for specimens preconditioned at 450°C as shown in Fig. 5. The maximum swelling rate occurred at ∿650°C. During irradiation at 735°C swelling decreased as the result of shrinkage of small voids. It was found that the dislocation density and void size distribution produced during neutron irradiation was virtually unchanged by nickel ion irradiations in the range 600–650°C, Fig. 6. Further swelling occurred through the continuing growth of preexisting voids,

without additional nucleation. The change in void size distribution which occurs when the neutron fluence is increased from $\sim 8 \times 10^{22}$ to $\sim 12 \times 10^{22}$ $n \cdot cm^{-2}$ is shown in Fig. 7. Also shown is the similar void size distribution change which occurs when specimens preconditioned at 450°C are Ni ion irradiated to a further 60 dpa at 650°C. The limited precipitate structure produced in-reactor was also maintained during ion irradiation, and it is concluded that these conditions represented an excellent simulation of in-reactor behavior. Since the maximum swelling rate occurred at ~650°C, the correct temperature shift required for correlation of neutron and ion swelling behavior appears to be ~200°C. Comparing the swelling rate in reactor at 450°C with the swelling rate under ion irradiation at 650°C we find that equal increments of void swelling are produced by 10 dpa (4 MeV Ni ions) and 10^{22} $n \cdot cm^{-2}$ ($E > 0.1$ MeV). Using this equivalence, the nickel ion data and neutron data may be superimposed, Fig. 8.

A similar set of nickel ion irradiations were carried out on specimens preconditioned at 585°C to 8×10^{22} $n \cdot cm^{-2}$. The additional swelling produced under nickel ion irradiation is shown plotted as a function of ion dose in Fig. 9. The behavior was radically different from that observed for the material preconditioned at 450°C, in that a decreasing swelling rate was observed at temperatures between 625 and 700°C. During the initial 30 dpa exposure at these temperatures, additional void nucleation occurred. However, after an irradiation to 60 dpa this population of small voids was no longer present. The large $M_{23}C_6$ particles, which developed in-reactor, dissolved during Ni ion irradiations at these temperatures and even after a dose of 30 dpa, the volume fraction was substantially reduced, Fig. 10. The eventual disappearance of the population of small voids is probably linked to the return of Ni and Si atoms to the matrix from the dissolving precipitates. For an ion irradiation temperature of 750°C, the neutron irradiated void number density and dislocation density

were maintained during ion irradiation, Fig. 11, and the swelling versus dose relationship extrapolated approximately back through the origin. The dissolution rate of $M_{23}C_6$ was significantly lower at this temperature and it appears that at this temperature conditions are approximately correct for a microstructural simulation of in-reactor behavior. The temperature shift is thus ∿180–200°C. In spite of this microstructural correlation, the actual rate at which swelling is proceeding is much lower than that observed for the 450°C preconditioned material, Fig. 12. The ratio of swelling rates at the reactor temperatures of 585 and 450°C is $R_n^{585}:R_n^{450} \approx 3:1$. The corresponding swelling rates for specimens ion irradiated at temperatures which preserve the in-reactor microstructures is $R_i^{650}:R_i^{750} = 1:3$. In other words, the ratio of peak temperature swelling rates observed in-reactor is not reproduced in ion irradiation of preconditioned specimens.

5. Discussion and Summary

During neutron irradiation, the point defect flow-induced segregation of solute atoms to internal sinks exerts a controlling influence over swelling. Segregation occurs through the migration of minor solute-defect complexes down point defect gradients and also by the preferential exchange of major solute alloying elements with vacancies. These processes occur over a wide range of temperatures and in the case of AISI 316, result in the formation of the Ni_3Si γ' phase below 500–520°C and the formation of a Ni and Si rich $M_{23}C_6$ phase at higher temperatures. Swelling behavior is modified by the depletion of Ni and Si from the matrix and also through the provision of sites for the nucleation of helium bubbles which are subsequently transformed into voids. At the displacement rates used for heavy ion irradiations (10^{-3}–10^{-2})dpa s^{-1} these segregation-precipitation processes in AISI 316 are inhibited by displacement cascade dissolution and γ' is not formed and very little carbide precipitation

occurs. During Ni ion irradiation very little change occurs in matrix chemistry and even with simultaneous helium injection, the precipitate-void complexes, characteristic of high temperature neutron irradiation, do not develop. Nickel ion irradiations at high damage rates produce an incomplete simulation of in-reactor behavior; and it is probably unwise to try to predict the in-reactor temperature or dose dependence of swelling from heavy ion data.

It was hoped to overcome the phase instability problem by using preconditioned specimens in which the in-reactor steady state matrix chemistry and phase distribution were established prior to nickel ion irradiation. However, this steady-state situation could not be maintained under ion irradiation, and both the γ' and $M_{23}C_6$ phases dissolved rapidly. This is principally a radiation effect since in some instances the ion irradiation temperatures were only 25°C higher than the neutron irradiation temperature. On the other hand, the void and dislocation structures established in reactor were maintained in ion irradiation experiments carried out at a temperature ∿200°C above the reactor temperature. However, the ratio of swelling rates in-reactor at 450 and 585°C could not be reproduced in the nickel ion irradiations. The swelling rate of the material preconditioned at 585°C was in fact too low by an order of magnitude. There are probably three factors contributing to the low swelling rate of the material preconditioned at 585°C.

a. The dissolution of the $M_{23}C_6$ phase results in an increase in matrix solute content.

b. At the high ion temperatures ∿750°C required to simulate in-reactor microstructural evolution at 585°C, continuous generation of helium is probably necessary to counteract vacancy loss by thermal emission.

c. Above 750°C, the proximity of the specimen surface probably begins to influence void growth.

In summary, predictions of the in-reactor temperature dependence of swelling rate from heavy ion irradiation experiments are generally unrealistic because of the complex dependence of phase stability on damage rate and alloy composition. For the same reasons, it is probably unwise to select alloy compositions for in-reactor performance on the basis of their behavior in ion irradiations. On the other hand, because of the good temperature control and rapidity of operation, heavy ion irradiations, properly used, are capable of providing the basic informations required for an understanding of (a) the effects of composition and damage rate on phase relationships under irradiation and (b) the complexities of the interaction between helium and certain phases in promoting high temperature swelling.

6. References

[1] Garner, F. A., Powell, R. W., Diamond, S., Lauritzen, T., Rowcliffe, A. F., Sprague, J. A., and Keefer, D., *International Conference on Radiation Effects in Breeder Reactor Structural Materials*, Scottsdale, Arizona, June 1977.

[2] Brager, H. R., and Garner, F. A., *J. Nucl. Mater.* 73 (1978) 9–19.

[3] Appleby, W. K., Bloom, E. E., Flinn, J. E., and Garner, F. A., *International Conference on Radiation Effects in Breeder Reactor Structural Materials*, Scottsdale, Arizona, June 1977.

[4] Bramman, J. J., Brown, C., Watkin, J. S., Cawthorne, C., Fulton, E. J., Barton, P. J., and Little, E. A., *International Conference on Radiation Effects in Breeder Reactor Structural Materials*, Scottsdale, Arizona, June 1977.

[5] Weiss, B., and Stickler, R., *Met. Trans.* 3 (1979) 851.

[6] Lam, N. Q., Okamoto, P. R., and Wiedersich, H., *J. Nucl. Mater.* 74 (1978) 101.

[7] Marwick, A. D., *J. Phys. F*, in press.

Table 1. Alloy Compositions (wt %)

Alloy	Fe	Cr	Ni	Mo	Si	Ti	Mn	C	N	S	P
316 (M2783)	65.8	16.8	13.0	2.5	0.47	<0.02	1.8	0.06	0.03	0.02	0.03

Table 2. Microstructural Data of Neutron Irradiated Solution Annealed AISI 316 (Heat M2783)

Specimen Ident.	Neutron Irrad. Temp (°C)	Neutron Fluence ($\times 10^{22}$n/cm^2)	Aver. Void Diam. (nm)	Void Number Density (#/cm^3)	(ΔV/V) TEM (%)	(Δp/p) (%)	Dislocation Density (cm/cm^3)	Precipitate Number Density (#/cm^3)
LP2D-D4	451	7.6	36.3	$\sim 3.5 \times 10^{14}$	$\sim$1.05	2.0	-	-
LP2D-D4-1G	451	7.6	30.8	8.2×10^{14}	1.56	2.0	6×10^{10}	-
LP2C-D1	445	12.5	45.4	8.1×10^{14}	6.1	6.5	-	-
LP2C-D1	445	12.5	47.4	7.9×10^{14}	6.0	6.5	-	-
LP2H-D4	520	7.6	56.5	3.2×10^{13}	(0.41 ± 0.07)	1.2	9.2×10^{9}	1.4×10^{13}
LP2H-D4-3A	520	7.6	50.6	1.1×10^{14}	1.03	1.2	3.7×10^{10}	-
LP2G-D1	516	12.5	62.5	4.6×10^{14}	12.1	5.7	-	-
LP2O-D1	584	8.1	128.0	2.3×10^{13}	(4.86 ± 0.72)	5.2	4.7×10^{9}	1.0×10^{13}
LP2O-D1-2C	584	8.1	109.0	3.2×10^{13}	2.98	5.2	5.0×10^{9}	-
LP2K-D1	560	12.5	176.0	3.1×10^{13}	13.5	18.4	-	-
LP2R-D1	665	12.5	237.5	1.3×10^{12}	2.2	2.4	-	-

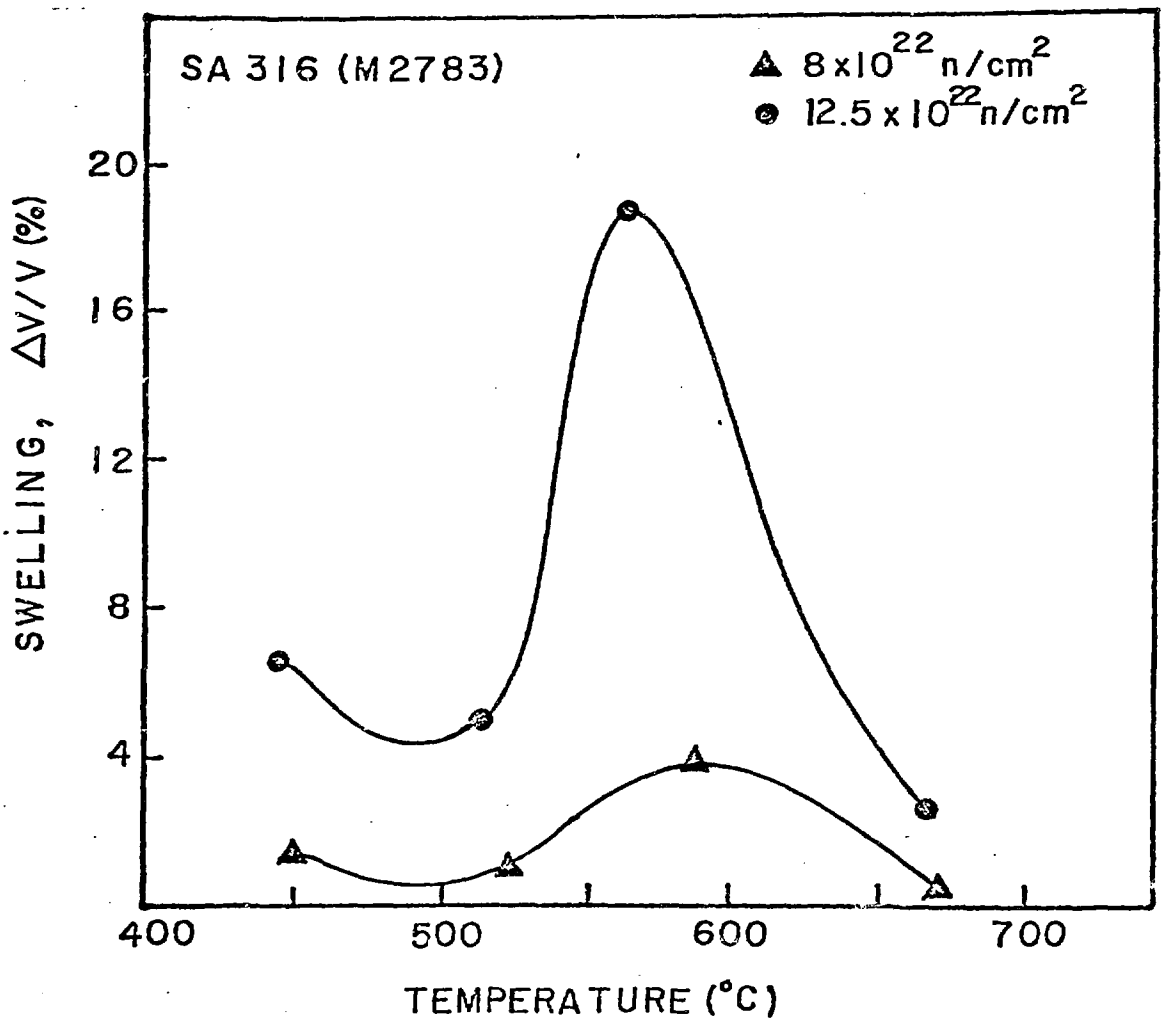

Fig. 1. Profilometry Swelling Data as a Function of Irradiation Temperature for the M2783 Heat of SA 316. (Ref. 3).

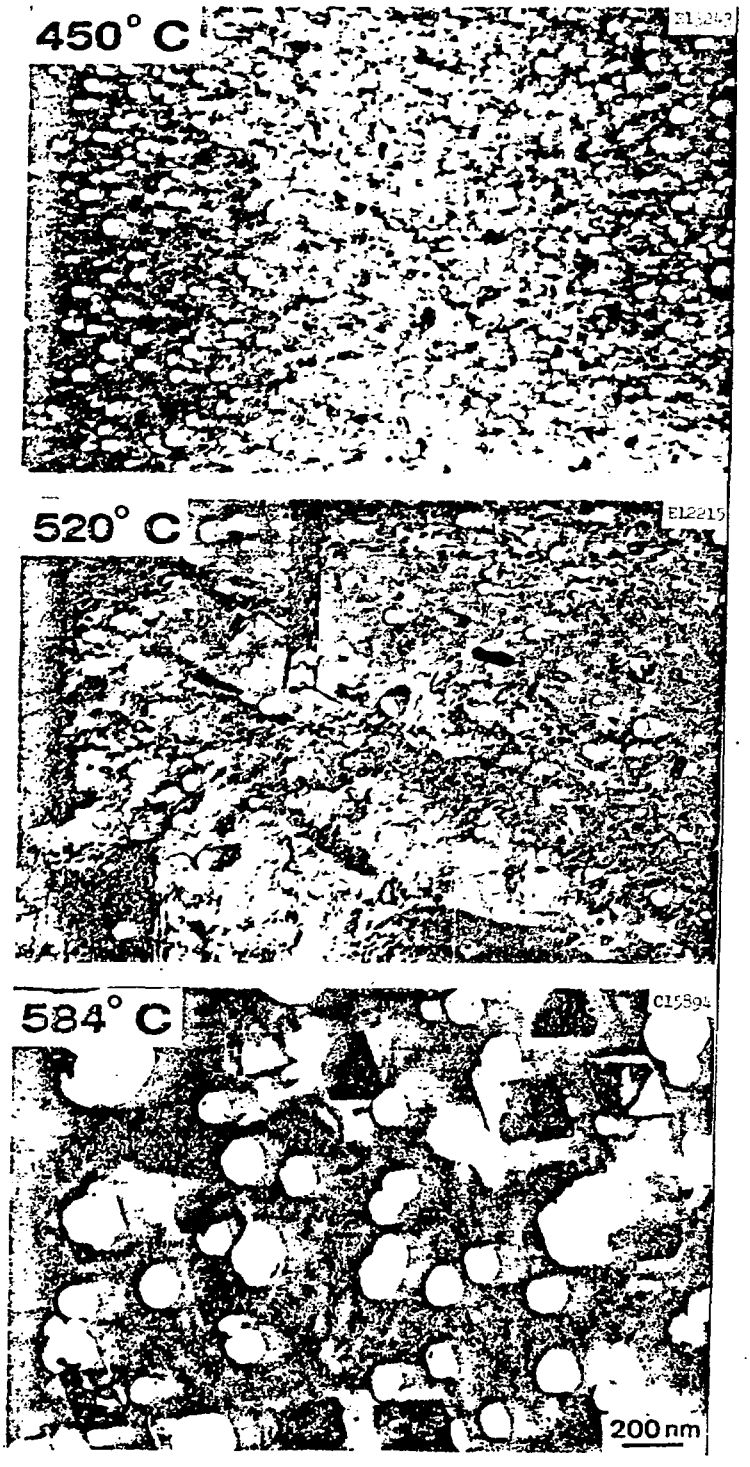

Fig. 2. TEM Micrographs of SA 316 Neutron Irradiated to ~8 × 10^{22} n·cm^{-2} at Three Temperatures.

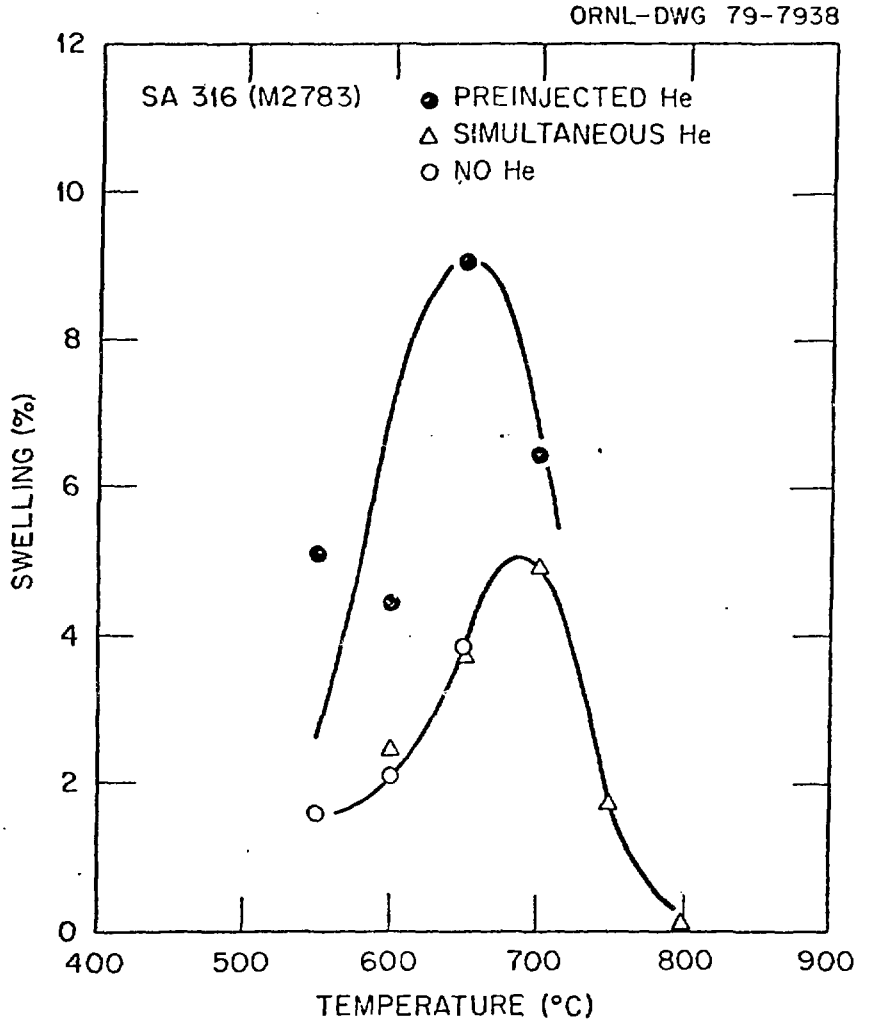

Fig. 3. Swelling as a Function of Temperature for SA 316 Stainless Steel Irradiated with 4 MeV Ni Ions to a Peak Displacement Dose of 100 dpa.

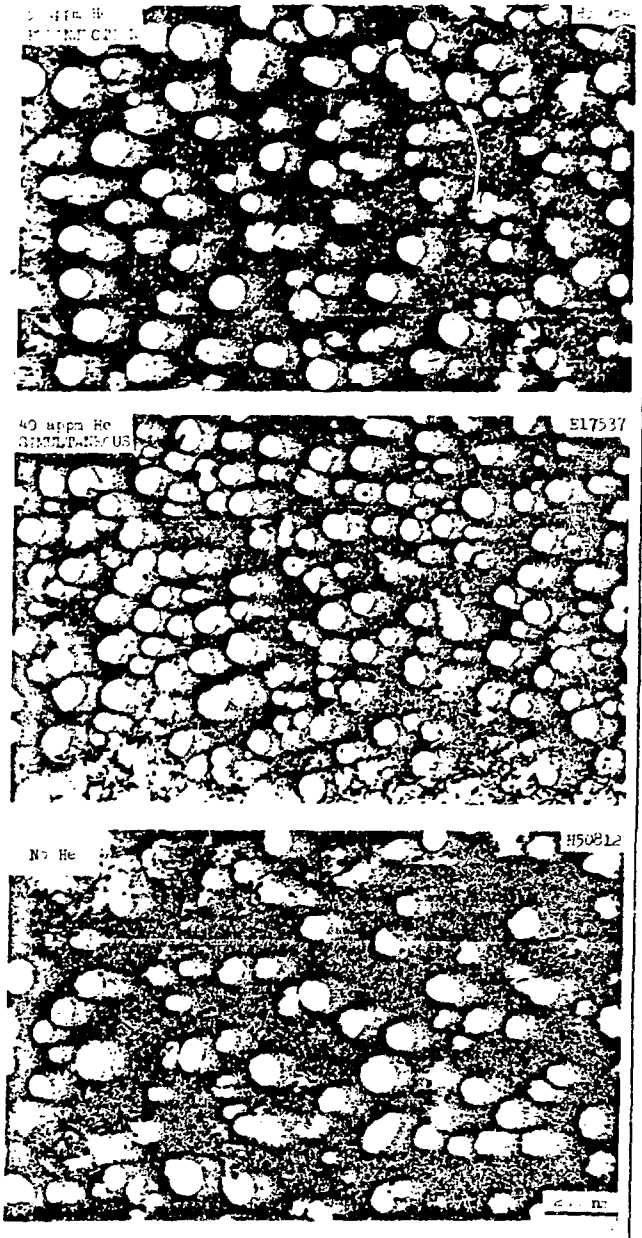

Fig. 4. TEM Micrographs of SA 316 Irradiated with 4 MeV Ni Ions to a Dose of 100 dpa at 650°C.

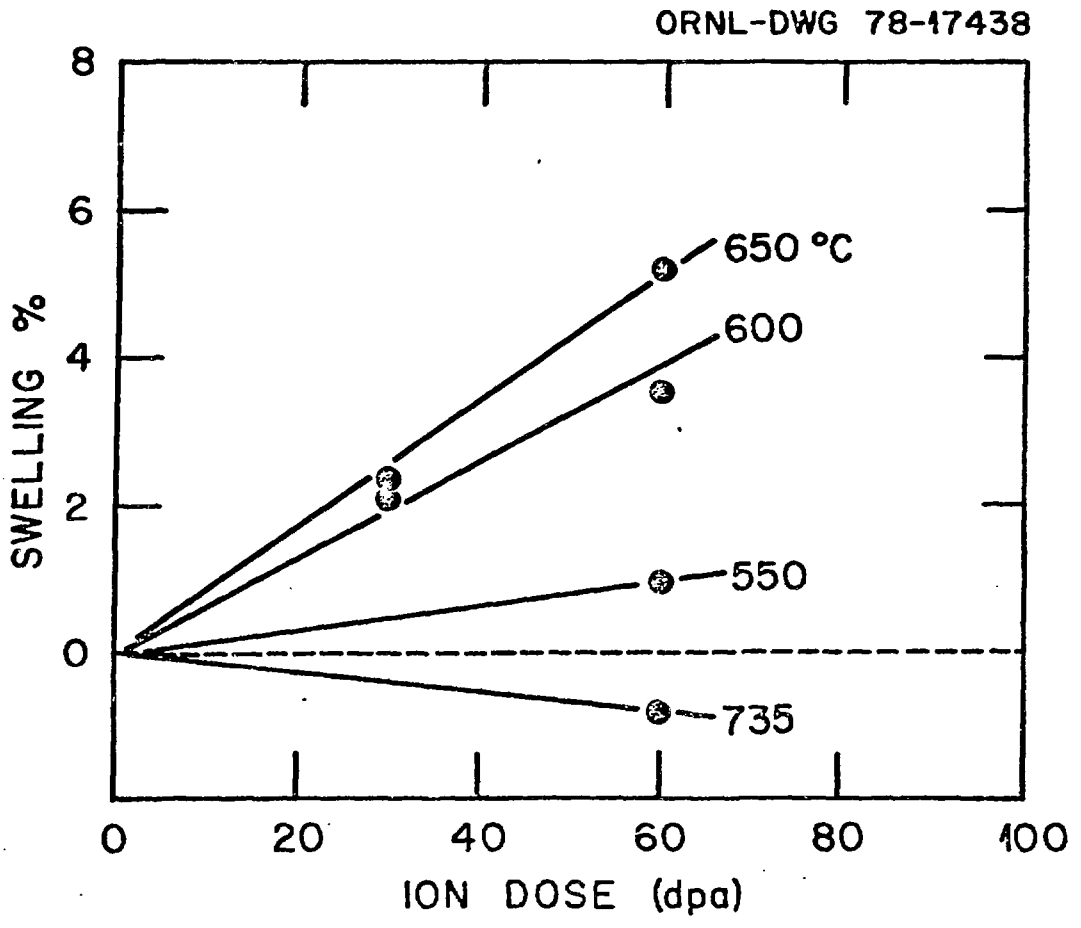

Fig. 5. Swelling as a Function of Dose for SA 316 Preconditioned at 450°C and Ni Ion Irradiated at Various Temperatures.

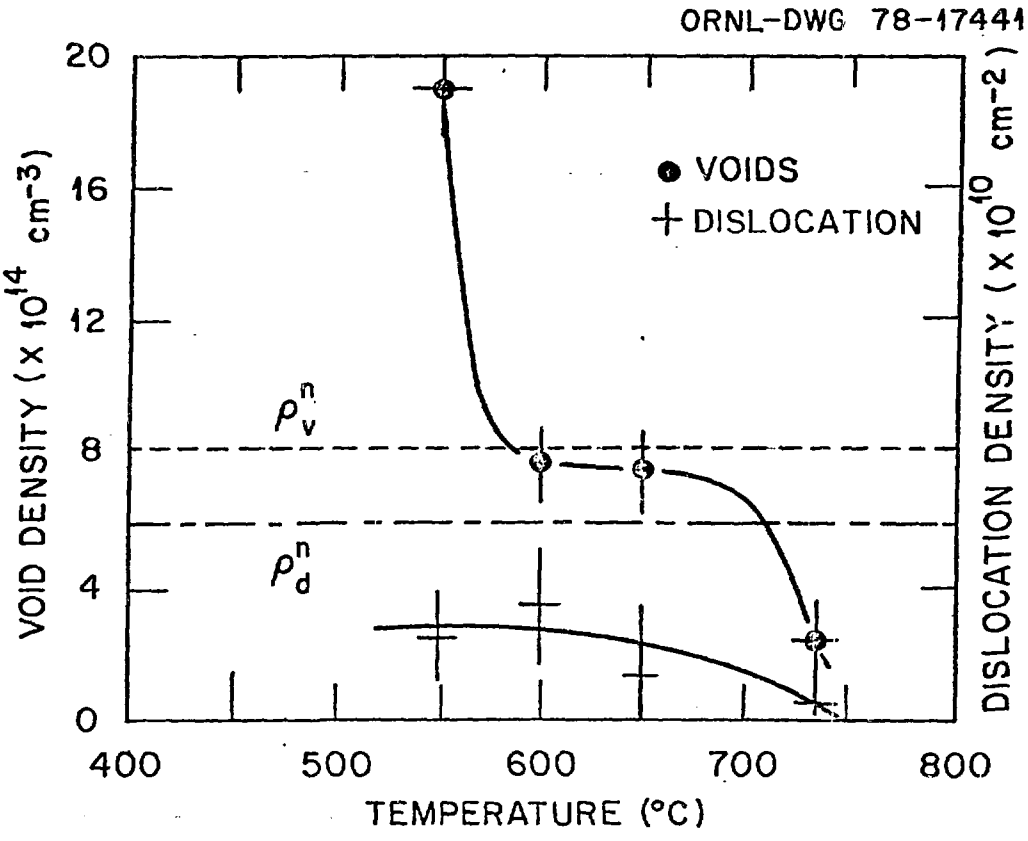

Fig. 6. Void Number Density and Dislocation Density in SA 316 Preconditioned at 450°C and Ni Ion Irradiated to a further 60 dpa. The broken horizontal lines indicate the neutron irradiated values.

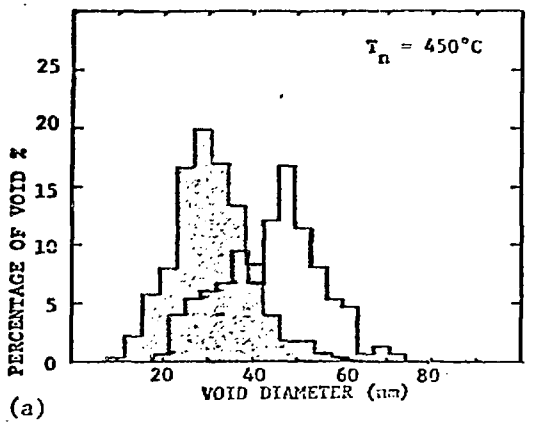

(a)

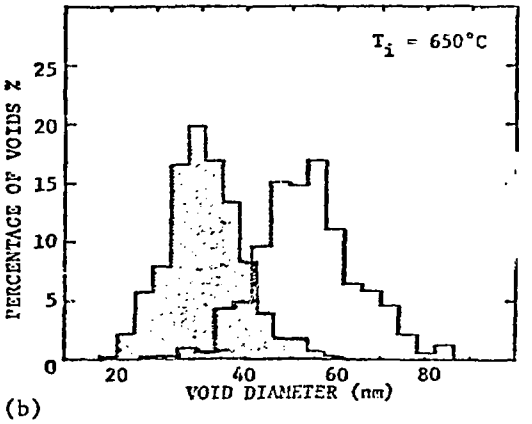

(b)

Fig. 7. Void Size Distribution Changes in Neutron Irradiated SA 316 After Neutron Irradiation to 8×10^{22} n·cm^{-2} (Shaded Area). (a) Further neutron irradiation to $\sim 12 \times 10^{22}$ n·cm^{-2} and (b) Further Ni ion irradiation to 60 dpa.

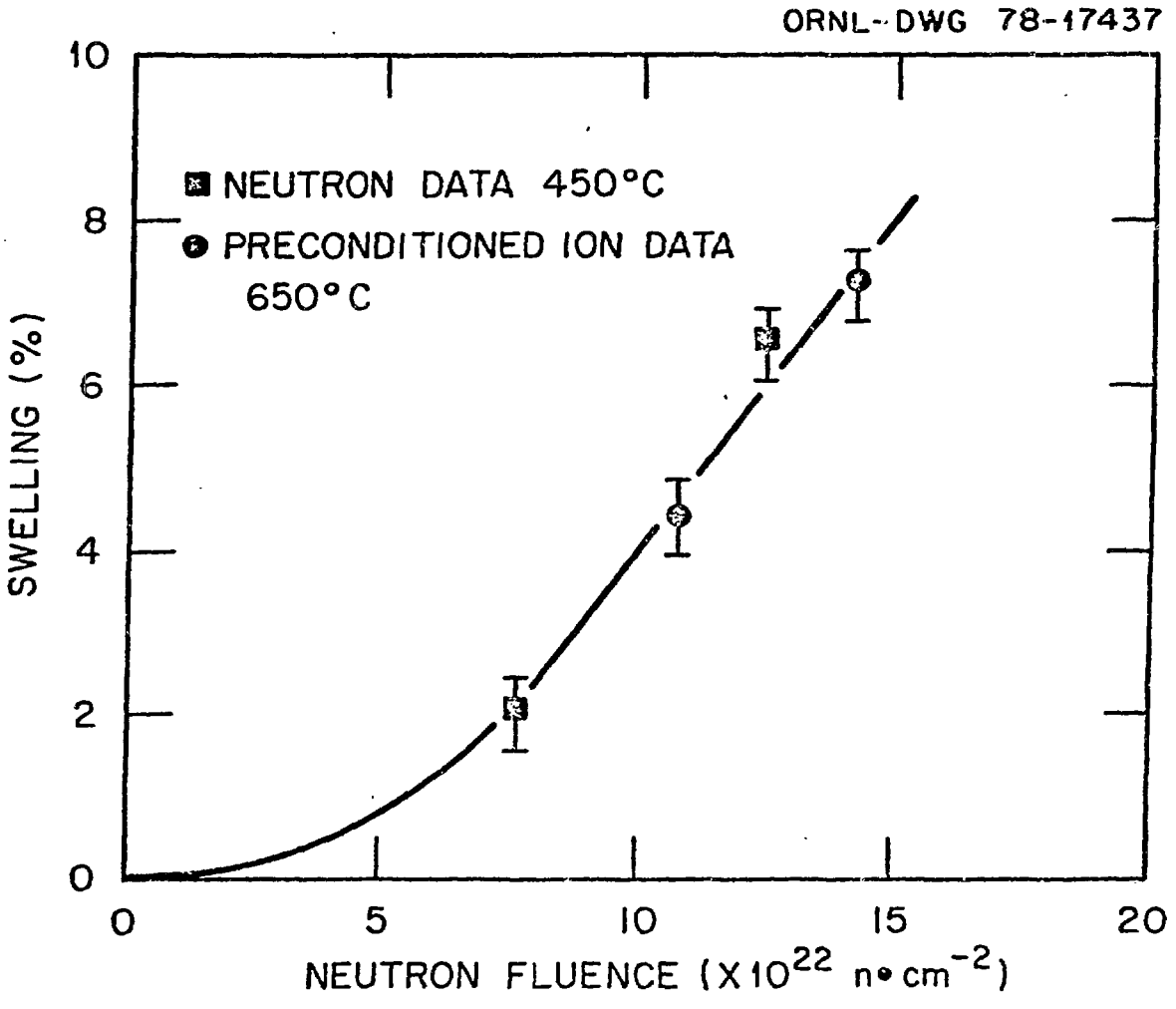

Fig. 8. Neutron and Ion Swelling Data Correlated on the Basis of an Equivalence of 10 dpa (Ni Ions) and 10^{22} $n \cdot cm^{-2}$ ($E > 0.1$ MeV).

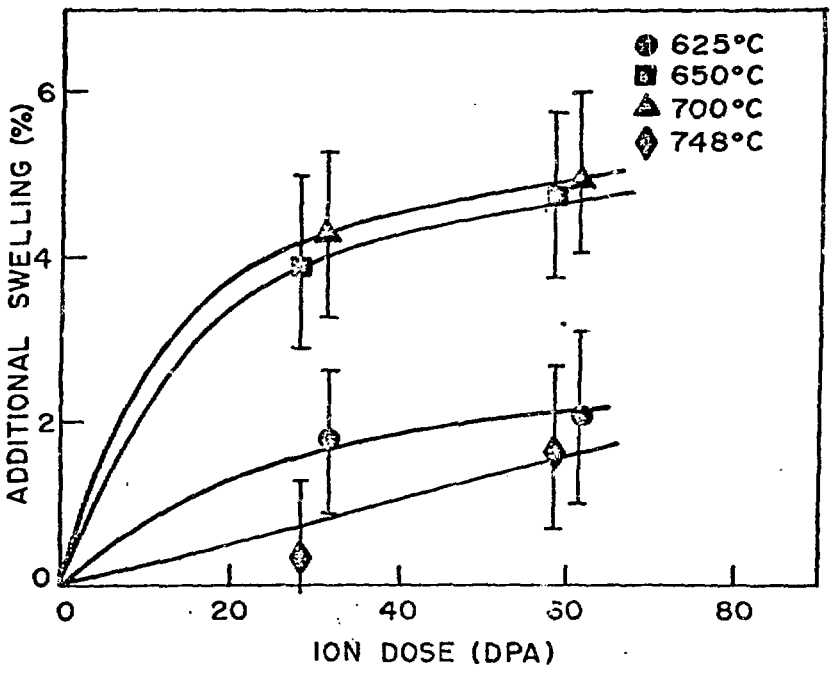

Fig. 9. Swelling as a Function of Dose for SA 316 Preconditioned at 585°C and Ni Ion Irradiated at Various Temperatures.

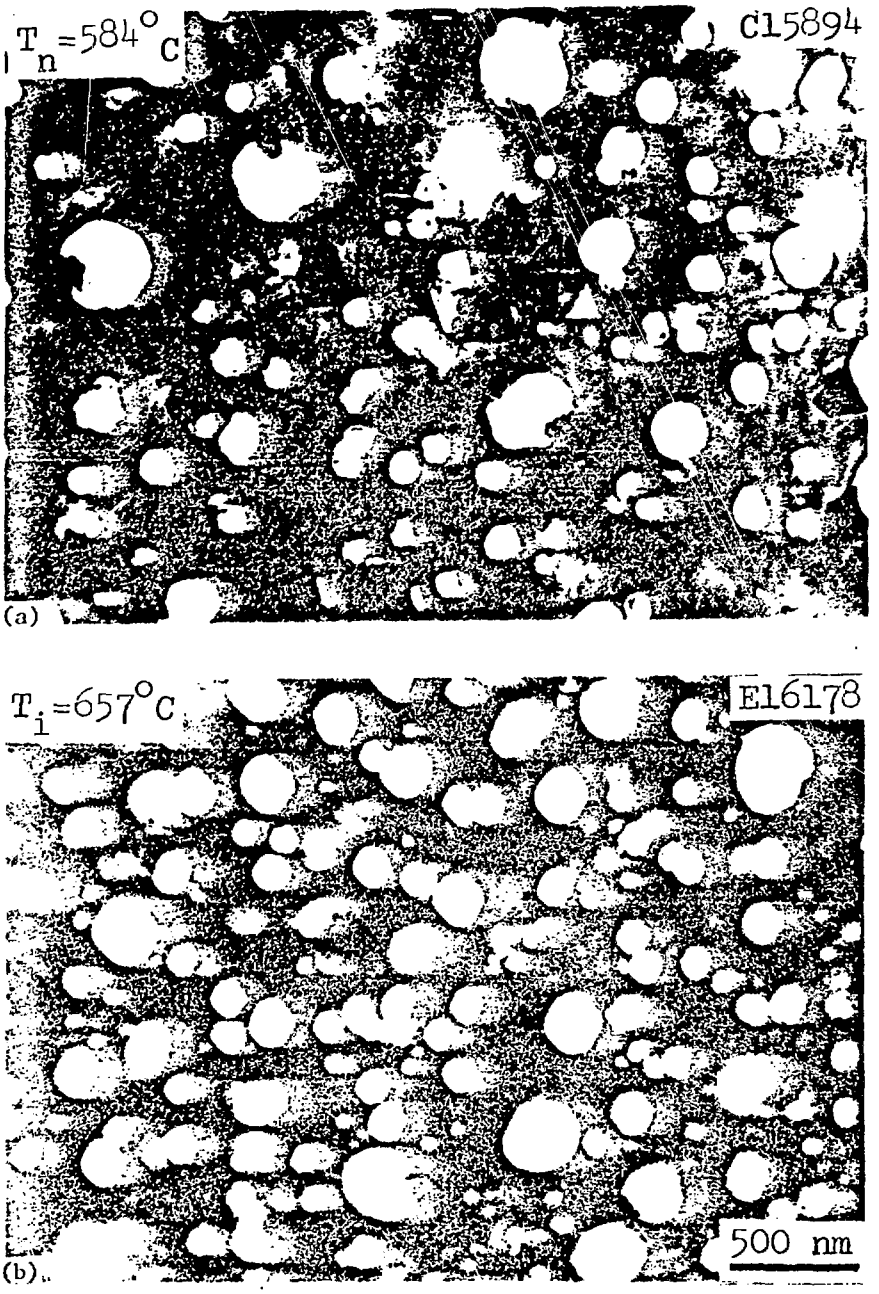

Fig. 10. TEM Micrographs of SA 316 (a) Neutron Irradiated at 584°C to 8 × 10^{22} n·cm^{-2} and (b) After Further Irradiation with 4 MeV Ni ions to 30 dpa at 657°C.

ORNL-DWG. 78-14694

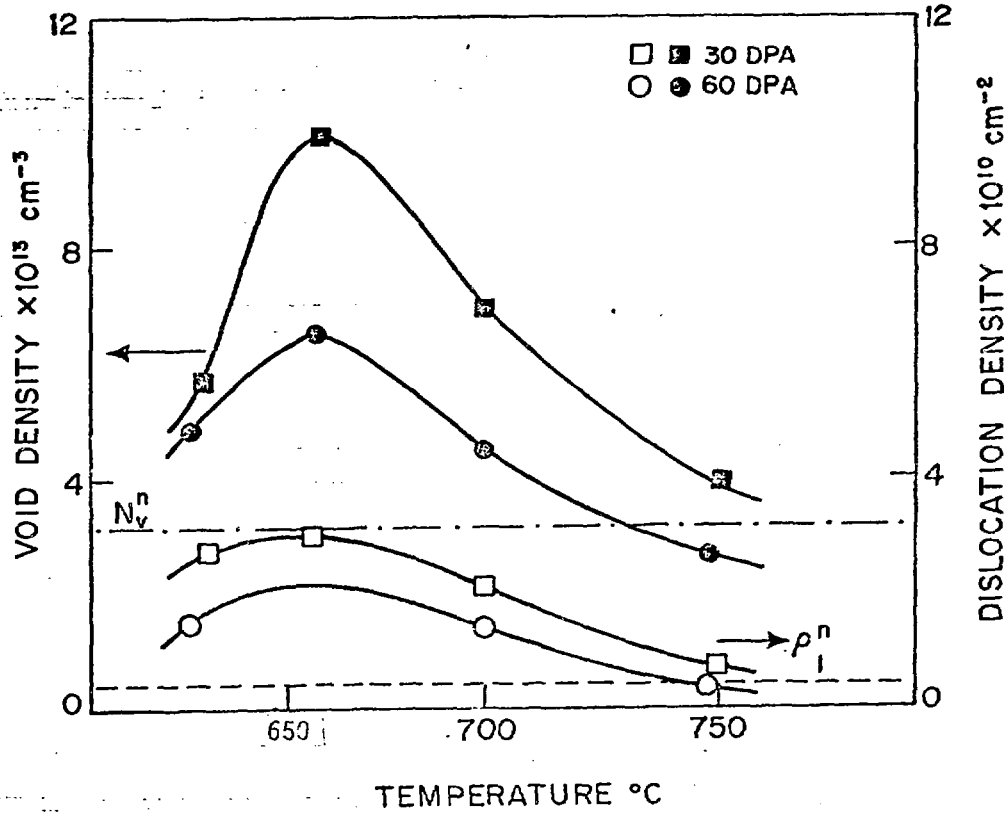

Fig. 11. Void Number Density and Dislocation Density in SA 316 Preconditioned at 585°C and Ni Ion Irradiated to 30 and 60 dpa. The broken horizontal lines indicate the neutron irradiated values.

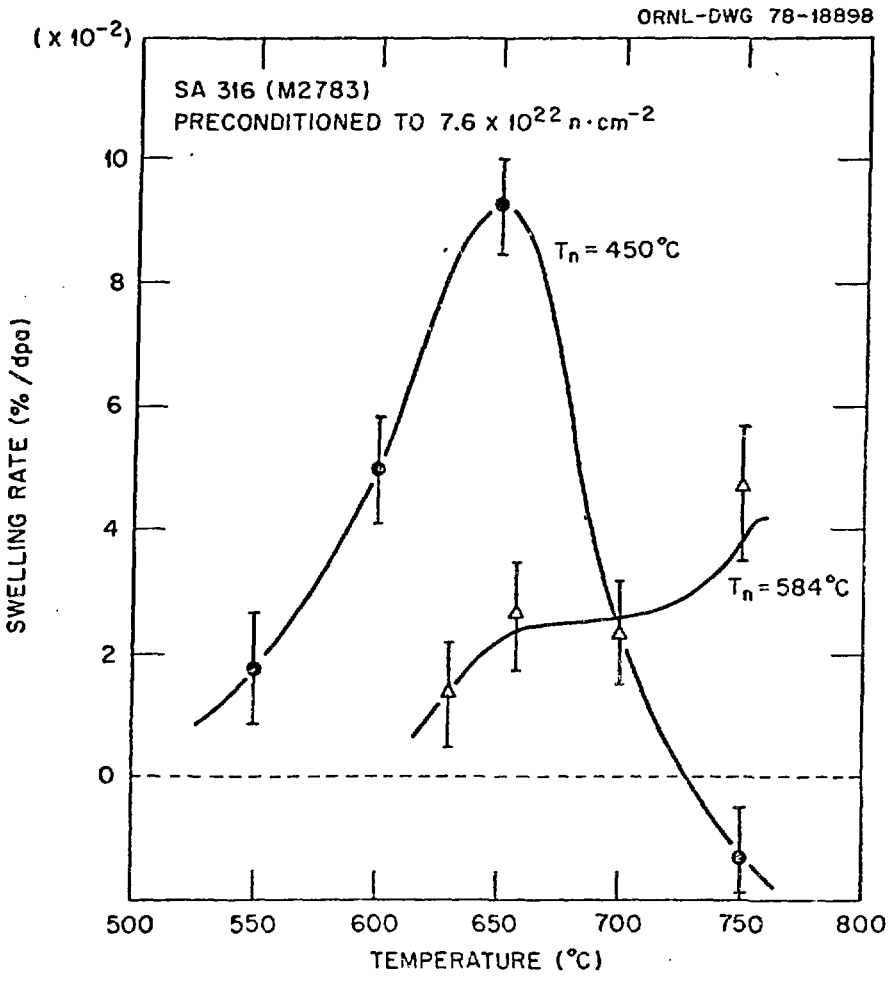

Fig. 12. Swelling Rate as a Function of Ni Ion Irradiation Temperature for SA 316 Preconditioned at 450°C and 584°C.